Accepted Manuscript

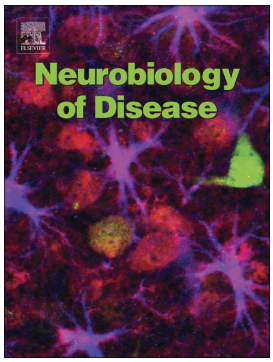

Normalizing the gene dosage of Dyrk1A in a mouse model of Down syndrome rescues several Alzheimer's disease phenotypes

Susana García-Cerro, Noemí Rueda, Verónica Vidal, Sara Lantigua, Carmen Martínez-Cué

PII: S0969-9961(17)30138-9
DOI: doi: 10.1016/j.nbd.2017.06.010
Reference: YNBDI 3980

To appear in: *Neurobiology of Disease*

Received date: 10 December 2016
Revised date: 30 May 2017
Accepted date: 20 June 2017

Please cite this article as: Susana García-Cerro, Noemí Rueda, Verónica Vidal, Sara Lantigua, Carmen Martínez-Cué , Normalizing the gene dosage of Dyrk1A in a mouse model of Down syndrome rescues several Alzheimer's disease phenotypes, *Neurobiology of Disease* (2017), doi: 10.1016/j.nbd.2017.06.010

This is a PDF file of an unedited manuscript that has been accepted for publication. As a service to our customers we are providing this early version of the manuscript. The manuscript will undergo copyediting, typesetting, and review of the resulting proof before it is published in its final form. Please note that during the production process errors may be discovered which could affect the content, and all legal disclaimers that apply to the journal pertain.

ACCEPTED MANUSCRIPT

Normalizing the gene dosage of *Dyrk1A* in a mouse model of Down syndrome rescues several Alzheimer's disease phenotypes

Susana García-Cerro[1], Noemí Rueda[2], Verónica Vidal[2], Sara Lantigua[2], Carmen Martínez-Cué[2]*

[1] Department of Anatomical Pathology, Pharmacology and Microbiology. Faculty of Medicine, University of Barcelona, Barcelona, Spain

[2] Department of Physiology and Pharmacology. Faculty of Medicine, University of Cantabria, Santander, Spain

* Corresponding author. email: martinec@unican.es

Abstract

The intellectual disability that characterizes Down syndrome (DS) is primarily caused by prenatal changes in central nervous system growth and differentiation. However, in later life stages, the cognitive abilities of DS individuals progressively decline due to accelerated aging and the development of Alzheimer's disease (AD) neuropathology. The AD neuropathology in DS has been related to the overexpression of several genes encoded by Hsa21 including *DYRK1A* (dual-specificity tyrosine-(Y)-phosphorylation regulated kinase 1A), which encodes a protein kinase that performs crucial functions in the regulation of multiple signaling pathways that contribute to normal brain development and adult brain physiology. Studies performed *in vitro* and *in vivo* in animal models overexpressing this gene have demonstrated that the *DYRK1A* gene also plays a crucial role in several neurodegenerative processes found in DS. The Ts65Dn (TS) mouse bears a partial triplication of several Hsa21 orthologous genes, including *Dyrk1A*, and replicates many DS-like abnormalities, including age-dependent cognitive decline, cholinergic neuron degeneration, increased levels of APP and Aβ, and tau hyperphosphorylation. To use a more direct approach to evaluate the role of the gene dosage of *Dyrk1A* on the neurodegenerative profile of this model, TS mice were crossed with *Dyrk1A* KO mice to obtain mice with a triplication of a segment of Mmu16 that includes this gene, mice that are trisomic for the same genes but only carry two copies of *Dyrk1A*, euploid mice with a normal *Dyrk1A* dosage, and CO animals with a single copy of *Dyrk1A*. Normalizing the gene dosage of *Dyrk1A* in the TS mouse rescued the density of senescent cells in the cingulate cortex, hippocampus and septum, prevented cholinergic neuron degeneration, and reduced App expression in the hippocampus, Aβ load in the cortex and hippocampus, the expression of phosphorylated tau at the Ser202 residue in the hippocampus and cerebellum and the levels of total tau in the cortex, hippocampus and cerebellum. Thus, the present study provides further support for the role of the *Dyrk1A* gene in several AD-like phenotypes found in TS mice and indicates that this gene could be a therapeutic target to treat AD in DS.

Keywords: *Dyrk1A*, senescence, neurodegeneration, APP, tau, Ts65Dn, Down syndrome

Highlights:

Dyrk1A is implicated in several Alzheimer's Disease phenotypes found in Down syndrome

Reducing *Dyrk1A* gene dosage in Ts65Dn mice rescued cellular senescence

Reducing *Dyrk1A* gene dosage in Ts65Dn mice prevented cholinergic neurodegeneration

Normalizing *Dyrk1A* copy number in Ts65Dn mice reduced Aβ load and App and tau levels

ACCEPTED MANUSCRIPT

Acknowledgements

This work was supported by the Jerome Lejeune Foundation, Fundación Tatiana Pérez de Guzmán el Bueno and the Spanish Ministry of Economy and Competitiveness (PSI-2016-76194-R, AEI/FEDER, EU). The authors wish to express their gratitude to Mariona Arbonés for providing *Dyrk1A+/- KO* mice and to Eva García Iglesias for technical assistance.

ACCEPTED MANUSCRIPT

ACCEPTED MANUSCRIPT

Introduction

Down syndrome (DS) is the most common genetic cause of intellectual disability (Shin *et al*., 2009) and is primarily caused by prenatal changes in central nervous system growth and differentiation (Lott, 2012; Haydar and Reeves, 2012). However, in later life stages, the cognitive abilities of DS individuals progressively decline due to accelerated aging and to the development of Alzheimer's disease (AD) neuropathology. The primary hallmarks of AD, such as the accumulation of amyloid plaques composed of β-amyloid (Aβ) peptides, neurofibrillary tangles (NFTs) formed by insoluble deposits of abnormally hyperphosphorylated tau, neuroinflammation, synapse and neuron loss and regional atrophy, are present in 100% of individuals with DS by the fourth decade of life (Wilcock and Griffin, 2013**;** Lott, 2012; Cenini *et al*., 2012; Sabbagh *et al*., 2011; Lott and Dierssen, 2010; Teipel and Hampel, 2006).

This high prevalence of AD neuropathology in DS has been partially related to the overexpression of several AD-related genes encoded by Hsa21. One of these genes is *APP* (Amyloid Precursor Protein) and its triplication in DS leads to an increase in the production of Aβ peptides. An imbalance between Aβ production and clearance leads to high levels of these peptides, causing their fast aggregation and deposition in plaques, which can induce other AD-associated neuropathologies such as the increase in oxidative stress, neuroinflammation, neuronal death and the acceleration of the decline in learning and memory (Wilcock, 2012; Sipos *et al*., 2007; Eikeleboom *et al*., 2006; Hardy, 2006; Hardy and Higgins 1992).

Among the other trisomic genes that have been implicated in the cognitive decline and AD-related neuropathology observed in DS individuals is dual-specificity tyrosine-(Y)-phosphorylation regulated kinase 1A (*DYRK1A*). This gene encodes a protein kinase that performs crucial functions in the regulation of cell proliferation and multiple signaling pathways (Guedj *et al*., 2012; Becker and Sippl, 2011) that contribute to normal brain development and adult brain physiology (Becker and Sippl, 2011; Tejedor and Hämmerle, 2011).

The *DYRK1A* gene also plays a crucial role in several neurodegenerative processes found in DS (Ferrer *et al*., 2005), such as cholinergic neurodegeneration, tau hyperphosphorylation and amyloid accumulation due to APP phosphorylation. Although the extra copy of *APP* and its overexpression seems to be the primary cause of amyloidosis in the DS brain, several studies have demonstrated that *DYRK1A* plays an important role in this process by interacting with APP. DYRK1A phosphorylates APP at Thr668 *in vitro* in cells of a mouse model that overexpresses the human *DYRK1A* gene (hBACtg*Dyrk1A*) (Ryoo *et al*., 2008). This phosphorylation facilitates the excision of APP by β-secretase 1 (*Beta-secretase 1*, BACE1) and γ-secretase, inducing an accumulation of the neurotoxic peptides Aβ40 and Aβ42 (Wegiel *et al*., 2011; Vingtdeux *et al*., 2005; Lee *et al*., 2003). Therefore, overexpression of DYRK1A hyperphosphorylates APP leading to a cascade of Aβ accumulation.

The first evidence of the role of *DYRK1A* in tauopathies came from several *in vitro* studies demonstrating that it phosphorylates at least 12 of tau residues including the threonine 212 (Thr212) (Park and Chung, 2013; Liu *et al*., 2008; Woods *et al*., 2001). In addition, there is evidence of its *in vivo* role in tau hyperphosphorylation in transgenic mice that overexpress *Dyrk1A* alone (Tg*Dyrk1A*) (Ryoo *et al*., 2007), in mice with a partial trisomy of a group of genes including *Dyrk1A* (such as the Ts65Dn mouse, see below) (Liu *et al*., 2008), in the transchromosomic mouse model Tc1 (Sheppard *et al*., 2012) and in the temporal cortex of DS individuals (Qian *et al*., 2013; Liu *et al*., 2008). These results indicate that *DYRK1A* overexpression contributes to the appearance of neurofibrillary tangles and their subsequent neurotoxicity (Park and Chung, 2013).

ACCEPTED MANUSCRIPT

Similar to what is found in AD, cholinergic neuron degeneration has a prominent role in the cognitive decline of DS. *In vitro* studies have revealed that reducing the protein expression of Dyrk1A in trisomic cells from the Ts65Dn mouse rescues the expression of *choline acetyltransferase* (ChAT) (Hijazi *et al*., 2013). Therefore, there is also evidence of the role of this gene in the cholinergic neuron degeneration found in DS.

As mentioned above, evidence for the role of *DYRK1A* in various DS phenotypes is partially derived from studies performed in several segmental trisomic mouse models of DS that overexpress different sets of orthologous genes of human chromosome 21 (Hsa21), including *Dyrk1A* (Rueda *et al*., 2012; Bartesaghi *et al*., 2011) and in transgenic mice overexpressing *DYRK1A* in artificial bacterial or yeast chromosomes or carrying extra copies of the corresponding murine cDNA (De la Torre *et al*., 2014; Ahn *et al*., 2006; Altafaj *et al*., 2001; Smith *et al*., 1997).

The most commonly used model of DS is the Ts65Dn (TS) mouse, which bears a partial triplication of several Hsa21 orthologous genes, including *Dyrk1A* (Sturgeon and Gardiner, 2011). TS mice replicate many DS-like abnormalities, including alterations in behavior, learning and memory, brain morphology and hypocellularity, neurogenesis, neuronal connectivity and electrophysiological and neurochemical processes (Rueda *et al*., 2012; Bartesaghi *et al*., 2011). Similar to DS individuals, the TS mouse also shows age-dependent cognitive decline and degeneration starting at the age of 6 months, including cholinergic and noradrenergic neuron degeneration, increases in the levels of APP protein and Aβ peptides and tau hyperphosphorylation (Millan Sanchez *et al*., 2012; Rueda *et al*., 2010; Netzer *et al*., 2010; Liu *et al*., 2008; Seo *et al*., 2005). However, these animals do not show amyloid plaques or neurofibrillary tangles. TS mice also present increased oxidative stress and inflammatory morphology, such as microglial activation in the hippocampus and in the medial septum (Corrales *et al*., 2014; 2013; Lockrow *et al*., 2011; 2009; Hunter *et al*., 2004).

Although there is strong evidence for the role of *Dyrk1A* in several AD phenotypes found in DS, most studies have been performed *in vitro* or in animal models overexpressing this gene. The aim of this study was to use a more direct approach to evaluate the role of the gene dosage of *Dyrk1A* on different neurodegenerative phenotypes found in the TS model of DS. To do this, in the present study, TS mice were crossed with *Dyrk1A* KO mice to obtain mice with a triplication of a segment of Mmu16 that includes this gene (TS +/+/+), mice that are trisomic for the same genes but only carry two copies of *Dyrk1A* (TS +/+/-), euploid (CO) mice containing a normal *Dyrk1A* dosage (CO +/+) and CO animals with a single copy of *Dyrk1A* (CO +/-). The effect of the different gene dosages of *Dyrk1A* was assessed on the cellular senescence, cholinergic neuron density, APP levels, Aβ load, and total and phosphorylated tau displayed by these animals in different brain structures.

ACCEPTED MANUSCRIPT

Methods

The University of Cantabria Institutional Laboratory Animal Care and Use Committee approved this study, and the protocols were performed in accordance with the Declaration of Helsinki and the European Communities Council Directive (86/609/EEC).

Experimental Animals

Mice were generated by repeatedly backcrossing B6EiC3Sn a/A-Ts(17<16>)65Dn (TS) females with C57BL/6Ei x C3H/HeSNJ (B6EiCSn) F1 hybrid males. The Robertsonian Chromosome Resource (The Jackson Laboratory, Bar Harbor, ME, USA) provided the parental generations, and mating was performed at the animal facilities of the University of Cantabria.

TS females were crossed with the *Dyrk1A*+/- heterozygous male mice breed on a mixed C57BL/6-129Ola genetic background (Fotaki *et al*., 2002) to obtain TS mice carrying a triplicated Mmu16 segment (TS +/+/+) extending from the Mrp139 gene to the Znf295 gene, including the *Dyrk1A* gene, mice trisomic for all of these genes but diploid for *Dyrk1A* (TS +/+/-), euploid (CO) mice containing a normal *Dyrk1A* dosage (CO +/+) and CO animals with a single copy of *Dyrk1A* (CO +/-).

To determine trisomy, the animals were karyotyped using real-time quantitative PCR (qPCR), as previously described (Liu *et al*., 2003). C3H/HeSnJ mice carry a recessive mutation that leads to retinal degeneration (Rd); therefore, all of the animals were genotyped using standard PCR to detect the *Rd* mutation (Bowes *et al*., 1993). Experiments were conducted using wt/wt or Rd1/wt animals. The *Dyrk1A* dosage of the mice was genotyped using PCR, as previously described (Fotaki *et al*., 2002).

A total of 96 male mice were used (6 TS +/+/+, 6 TS +/+/-, 6 CO +/+ and 6 CO +/- of 5-6 months of age and 18 TS +/+/+, 18 TS +/+/-, 18 CO +/+ and 18 CO +/- of 13-14 months of age). Twelve animals from each group were used for the immunohistochemical detection of ChAT (6 of 5-6 months of age and 6 of 13-14 months of age). Six extra animals per group of mice 13-14 months of age were used for the senescence studies and 6 mice of the same age were used for the western blot and ELISA analyses. The researchers were blind to the genotype and karyotype throughout the entire assessment.

Histological and stereological procedures

Mice were deeply anesthetized with pentobarbital and transcardially perfused with saline, followed by 4% paraformaldehyde. After postfixation in 4% paraformaldehyde overnight at 4°C and transfer into 30% sucrose, the brains were frozen on dry ice and coronally sliced using a cryostat (50-µm-thick sections to examine the cingulate cortex and hippocampus and 30-µm-thick sections to examine the medial septum). Every eighth section throughout the rostrocaudal extent of the cingulate cortex and hippocampus and every sixth section of the medial septum were used.

Histochemical detection of senescence-associated β-galactosidase

The density of senescent cells in the cingulate cortex, the subgranular zone (SGZ), a narrow layer of cells located between the granule cell layer and hilus of the dentate gyrus (DG), the granular layer (GL) of the DG and the medial septum was estimated in the different groups of mice using the SA-β-gal assay (senescence-associated β-galactosidase) method according to He *et al*. (2013). Anatomical regions and their boundaries were identified according to the atlas of Paxinos and

ACCEPTED MANUSCRIPT

Watson (2007). The SA-β-gal staining background was used to define the anatomical structures (*e.g*. see images in **figure 1A**), and the Cavalieri method was employed to calculate the total area of the SGZ and the total volume of both the DG and medial septum, as previously described (Llorens-Martin et al, 2006). The volume of the cingulate cortex was not calculated, as this structure lacks clearly defined boundaries. Instead, anatomical landmarks were used to correctly position the dissector counting frames in this brain region.

Sections of the cingulate cortex, hippocampus and medial septum were washed twice with PBS and fixed for 15 min at room temperature with a 0.5% glutaraldehyde solution. Next, the sections were washed and incubated with a staining solution containing 5-bromo-4chloro-3-indolyl-β-D-galactopyranoside (X-gal, ThermoFisher Scientific, MA, USA) for 24 h at 37°C, mounted on Superfrost Plus glass slides, dehydrated, cleared, and coverslipped with mounting medium.

SA-β-gal-positive cells (showing a blue reaction product over the cell soma) were counted along the SGZ and on the GL of the DG of each animal using a Zeiss Axioskop 2 plus microscope with a 40X objective in one-in-eight series sections. To determine the senescence cell density in the SGZ, the total number of positive cells was divided by the area of the SGZ (defined as the length of the SGZ divided by the thickness of the section). To determine the GL density, the number of positive cells was divided by the volume of the GL in every section. The total number of SA-β-gal-positive cells in these structures was calculated using a variation of the optical dissector method, as previously described (Trejo et al., 2001). Briefly, the cell density was multiplied by the total volume of the GL or total SGZ extension previously estimated using the Cavalieri method.

The number of SA-β-gal-positive cells in the cingulate cortex and medial septum was quantified using a systematic random design of dissector counting frames (250 x 250 μm). Both anatomical structures were photographed using a Zeiss Axioskop 2 plus microscope with a 10X objective. In a one series of sections, six independent fields were randomly selected along the cingulate cortex and medial septum. The number of senescent cells was counted within each frame and divided by the dissector extension to estimate the cellular density. The values were averaged to calculate the density for each animal. For cell number quantification in the cingulate cortex, the cells were counted within a 0.0625-mm^2 area of the cingulate cortex. The total number of senescent cells in the medial septum was obtained after multiplying the cell density by the total extension of the region. Image analysis was performed using NIH ImageJ software (National Institutes of Health, MD, USA).

Immunocytochemical detection of ChAT

After inactivation of endogenous peroxidase for 30 min in 3% hydrogen peroxide, slices containing the medial septum were washed three times in phosphate-buffered saline (PBS) and blocked for 1 h in PBS containing 20% normal donkey serum (NDS) and 0.2% Triton X-100 prior to overnight incubation at room temperature (RT) in a mixture containing the primary antibody (goat polyclonal Anti-ChAT, Chemicon; 1:100). After rinsing the sections in PBS three times for 10 min each, the sections were incubated for 2 h in biotinylated secondary antibody (anti-goat, Vector Laboratories; 1:250) diluted in 2% NDS in PBS at RT. The sections were rinsed three times in PBS and incubated for 1 h at RT in a streptavidin-biotin complex (Vectastain ABC Kit) in PBS. Following a thorough rinsing with PBS, immunohistochemical staining was visualized by incubation in 3.3'-diaminobenzidine solution (Vector Laboratories). After immunostaining, floating tissue sections were mounted on Superfrost Plus glass slides, dehydrated, cleared, and coverslipped with mounting medium. The medial septum was photographed using a Zeiss Axioskop 2 plus

ACCEPTED MANUSCRIPT

microscope with a 10X objective, and all ChAT-positive cells were counted with NIH ImageJ Cell Counter software and divided by the area of the medial septum to calculate the density of this cell population. The total number of ChAT-positive cells was determined using a variation of the optical dissector method, as previously described (Trejo et al., 2001). Briefly, the cell density was multiplied by the total volume of the medial septum, estimated using the Cavalieri method as described in the previous section.

Western blotting

Mice were euthanized by decapitation and the cortex, hippocampus and cerebellum were dissected. Whole-cell lysates from the cortex, hippocampus and cerebellum were prepared as previously described (Rueda *et al*., 2010). The total protein content of each sample was determined using the method of Lowry *et al*. (1951). Identical amounts of total protein (50 µg) from each sample were loaded on a 10% sodium dodecyl sulfate-polyacrylamide gel, electrophoresed, and transferred to a polyvinylidene difluoride (PVDF) membrane (Bio-Rad, Hercules, CA, USA) using a Mini Trans-Blot Electrophoresis Transfer Cell (Bio-Rad). The efficient transfer of proteins was confirmed by staining the PVDF membrane with Ponceau red (Sigma-Aldrich, St. Louis, MO, USA). Non-specific binding of antibodies was prevented by incubating the membranes in TBST buffer (10 mM Tris-HCl, pH 7.6, 150 mM NaCl, 0.05% Tween 20) containing 3% bovine serum albumin (BSA). The blots were incubated with a mouse monoclonal anti-APP antibody (1:2000; Millipore, Billerica, MA, USA), mouse monoclonal anti-Tau5 antibody (1:1000; Millipore), rabbit monoclonal anti-Tau pSer202 antibody (1:100; Abcam Cambridge, United Kingdom), and a rabbit polyclonal anti-Tau pThr212 antibody (1:100; Invitrogen, Carlsbad, CA, USA) diluted in TBST containing 3% BSA overnight at 4°C. After extensive washing with TBST, the blots were incubated with a goat anti-mouse IRDye 800CW or a goat anti-rabbit IRDye 680RD antibody (1:10.000; LI-COR Biotechnology, Lincoln, Nebraska, USA) for 1 h at room temperature. The fluorescence was detected using a LI-COR ODYSSEY IR Imaging System V3.0 (LI-COR Biotechnology). The images were exported and saved as gray scale TIFF files (16 bit) to improve the contrast between signal and noise. Subsequently, the integrated optical density of the bands was determined with NIH ImageJ software and normalized to the background values. The relative variations between the bands of the four groups of experimental mice were calculated in the same experiment. Each individual sample was evaluated in at least three independent experiments. The values were within a linear range. To ensure equal loading, the blots were reproved using a mouse monoclonal anti-GAPDH antibody (6C5) (1:2000; Santa Cruz Biotechnology, Santa Cruz, CA, USA).

Quantification of Aβ1-42 in brain tissue by ELISA

Sandwich Aβ ELISA was used to measure cortex, hippocampal and cerebellar levels of Aβ1-42. Briefly, the tissue samples were weighed and homogenized in 8X cold 5 M guanidine hydrochloride buffer (pH 8.0) and incubated 3 h at RT. Samples were diluted with standard dilution buffer (1:10), and centrifuged at 16.000 g for 20 min at 4°C to remove insoluble material. The supernatant fraction was collected and stored at −80°C. To quantify Aβ levels supernatant fractions were analyzed using a well-established mouse Aβ142 ELISA kit (KMB 3441) following the manufacturer´s instructions.

All the analyses were always performed in duplicate. OD450 values were detected on a microplate reader (Multiskan EX, Thermo Electron Corporation). The Aβ1-42 levels were calculated according to the standard curve.

ACCEPTED MANUSCRIPT

Statistical analysis

Data were analyzed using a two-way ('karyotype' x 'Dyrk1A') ANOVA. The mean values for each experimental group were compared post hoc using Bonferroni tests. All of the analyses were performed using SPSS (version 22.0, Chicago, IL, USA) for Windows.

ACCEPTED MANUSCRIPT

ACCEPTED MANUSCRIPT

Results

Normalization of the *Dyrk1A* copy number normalized the density of cells with a senescent phenotype in the hippocampus and medial septum of TS mice

Cellular senescence is a process that contributes to the dysfunction of the aging brain. To evaluate the effects of the *Dyrk1A* copy number on this pathological process, we estimated the density of SA-β-gal-positive cells in the hippocampus, medial septum and cingulate cortex of the four experimental groups. TS +/+/+ mice presented an increased density of cells with a senescent phenotype in the GL (ANOVA 'karyotype': $F_{(1,21)}$=0.05, **figures 1A and 1B**), SGZ ($F_{(1,21)}$=1.26, **p=0.27; figures 1A and 1D**), medial septum ($F_{(1,21)}$=7.44, p=0.012; **figures 1F and 1D**), and cingulate cortex (**figures 1I and 1J**). Similar results were obtained in the analyses of total cell number. The number of cells undergoing senescence was higher in the GL (ANOVA 'karyotype': $F_{(1,21)}$=3.70, p=0.067, **figure 1C**), SGZ ($F_{(1,21)}$=7.015, p=0.007; **figure 1E**) and septum ($F_{(1,21)}$=11.43, p=0.003; **figure 1E**) of TS +/+/+ mice. In the cingulate cortex, ANOVA revealed no significant effect of 'karyotype' on the cell number ($F_{(1,21)}$=0.016, p=0.90; **figure 1K**). However, this result reflected the fact that both CO and TS mice were considered in this analysis, and the increase in the number of senescent cells in CO +/- mice compared to CO +/+ and the decrease in TS+/+/- compared to TS +/+/+ masked the difference between TS+/+/+ and CO +/+ animals. When the effect of gene manipulations on both genotypes was considered, TS +/+/+ mice displayed a higher number of senescent cells in the cingulate cortex than CO +/+ animals (ANOVA 'karyotype x Dyrk1A': $F_{(1,21)}$=10.63, p=0.004; **figure 1K**).

Reducing one copy of *Dyrk1A* rescued the reduction in the density of senescent cells in the hippocampus of TS +/+/- mice but had no effect in CO +/- mice (GL: 'Dyrk1A': $F_{(1,21)}$=0.47, p=0.49; ''karyotype' x 'Dyrk1A'': $F_{(1,21)}$=8.78, p=0.007, **figure 1B**; SGZ: 'Dyrk1A': $F_{(1,21)}$=1.43, p=0.24; ''karyotype' x 'Dyrk1A'': $F_{(1,21)}$=12.54, p=0.002, **figure 1D**). However, when the total number of cells was quantified in these structures, both TS and CO mice with reduced *Dyrk1A* copy numbers presented a reduction in the number of cells (GL: 'Dyrk1A': $F_{(1,21)}$=11.73, p=0.002; ''karyotype' x 'Dyrk1A'': $F_{(1,21)}$=0.44, p=0.51, **figure 1C**; SGZ: 'Dyrk1A': $F_{(1,21)}$=8.89, p=0.007; ''karyotype' x 'Dyrk1A'': $F_{(1,21)}$=1.46, p=0.024, **figure 1E**). The fact that the number of cells was lower in the CO +/- group than in the CO +/+ group reflects the well-documented reduction in hippocampal size observed in this group of animals (Guedj et al., 2012). However, when this measure was corrected after considering the area or volume of these areas, the animals showed normal cell densities, indicating that reducing a functional copy of this gene did not affect senescence in the CO +/- hippocampus.

In the septum, reducing one copy of *Dyrk1A* rescued the density of cells with a senescent phenotype ('Dyrk1A': $F_{(1,21)}$=28.90, p<0.001; ''karyotype' x 'Dyrk1A'': $F_{(1,21)}$=0.32, p=0.58; **figure 1G**) and decreased the total number of cells undergoing senescence ('Dyrk1A': $F_{(1,21)}$=34.48, p=0.001; ''karyotype' x 'Dyrk1A'': $F_{(1,21)}$=2.66, p=0.11; **figure 1G**) in both TS +/+/a and CO +/- mice.

Moreover, in the cingulate cortex, reducing a functional copy of *Dyrk1A* in TS +/+/- but not in CO +/- mice reduced the density ('Dyrk1A': $F_{(1,21)}$=0.31, p=0.58; ''karyotype' x 'Dyrk1A'': $F_{(1,21)}$=9.06, p=0.007; **figure 1J**) and number ('Dyrk1A': $F_{(1,21)}$=0.75, p=0.39; ''karyotype' x 'Dyrk1A'': $F_{(1,21)}$=10.63, p=0.004; **figure 1K**) of senescent cells. Although it is likely that CO +/- mice might also present a reduction in the size of the cingulate cortex, and thus a normal density of senescent cells, the volume of this structure was not calculated, as the cingulate cortex lacks clearly defined boundaries. As explained in the methods section, anatomical landmarks were used to correctly

ACCEPTED MANUSCRIPT

position dissector counting frames in this brain region, and the cells were counted within a 0.0625-mm^2 area of the cingulate cortex.

Therefore, *Dyrk1A* may protect mice from the development of cell senescence in CO mice in the medial septum and TS mice in the medial septum, cingulate cortex and hippocampus.

Normalizing *Dyrk1A* gene dosage prevented cholinergic neurodegeneration in trisomic animals

The septum of TS mice is characterized by a progressive cholinergic degeneration. To investigate the relationship between this process and the *Dyrk1A* copy number, we performed a quantitative analysis of the density of ChAT-positive cells in this structure. At 6 months of age, the density (ANOVA 'karyotype'; $F_{(1,21)}$=0.34, p=0.56; **figures 2A and 2C**) or the total number of cells ($F_{(1,21)}$=1.89, p=0.18; **figures 2A and 2E**) with a cholinergic phenotype in the septum of TS +/+/+ did not significantly differ from that in the other groups of animals. In addition, reducing one functional copy of *Dyrk1A* did not modify the density ('Dyrk1A': $F_{(1,21)}$=1.46, p=0.25; ''karyotype' x 'Dyrk1A'': $F_{(1,21)}$=0.03, p=0.86; **figures 2A and 2C**) or the total number ('Dyrk1A': $F_{(1,21)}$=2.31, p=0.14; ''karyotype' x 'Dyrk1A'': $F_{(1,21)}$=1.54, p=0.23; **figures 2A and 2E**) of ChAT+ cells in this structure.

However, 13-14-month-old TS +/+/+ mice presented a marked reduction in the density of this population of cells (ANOVA 'karyotype': $F_{(1,21)}$=9.71, p=0.005; **figures 2B and 2D**). Reducing the *Dyrk1A* gene copy number completely rescued this deficit in 13-14-month old TS +/+/- mice ('Dyrk1A': $F_{(1,21)}$=10.074, p=0.004; **figures 2B and 2D**), without having any effect in CO +/- animals ('karyotype' x 'Dyrk1A''): $F_{(1,21)}$=8.48, p=0.008). In addition, TS +/+/+ and CO +/- mice presented a reduction in the total number of ChAT+ cells, which was not rescued in TS +/+/- mice (ANOVA 'karyotype': F(1,21)=0.18, p=0.67; 'Dyrk1A': $F_{(1,21)}$=5.0, p=0.035; 'karyotype x Dyrk1A': F(1,21)=7.93, p=0.010; **figures 2B and 2F**). The discrepancies between the density and total number of cells observed in the different groups of aged animals likely reflect differences in the size of the septum, as previously observed in other brain areas in CO +/- mice.

These results suggest that the overexpression of *Dyrk1A* plays a significant role in the reduction of cholinergic neuron density observed in TS +/+/+ animals.

ACCEPTED MANUSCRIPT

The reduction in *Dyrk1A* gene dosage decreased APP protein expression in the hippocampus of TS mice and in the cortex, hippocampus and cerebellum of CO mice

TS mice are also characterized by an enhancement in APP expression. Numerous studies have shown the regulatory role of *Dyrk1A* on APP processing and its scission of amyloid peptides. Therefore, we evaluated whether the gene dosage of *Dyrk1A* affects the APP protein levels in the cortex, hippocampus and cerebellum. As expected, TS +/+/+ mice presented enhanced levels of APP protein expression in the cortex (ANOVA 'karyotype': $F_{(1,21)}$=34.93, p<0.001; **figure 3A**), hippocampus ($F_{(1,21)}$=29.35, p<0.001; **figure 3B**) and cerebellum ($F_{(1,21)}$=7.23, p=0.014; **figure 3C**). Reducing the *Dyrk1A* copy number decreased the levels of this protein in mice of both karyotypes in all structures (cortex: 'Dyrk1A': $F_{(1,21)}$=6.96, p=0.010; ''karyotype' x 'Dyrk1A'': $F_{(1,21)}$=0.00, p=0.99; hippocampus: 'Dyrk1A': $F_{(1,21)}$=12.84, p=0.001; ''karyotype' x 'Dyrk1A'': $F_{(1,21)}$=0.25, p=0.61; cerebellum: 'Dyrk1A': $F_{(1,21)}$=5.51, p=0.029; ''karyotype' x 'Dyrk1A'': $F_{(1,21)}$=0.09, p=0.76), although this effect was more evident in all structures in CO +/- mice and in the hippocampus of TS +/+/- mice.

Normalization of the *Dyrk1A* copy number in TS +/+/- mice reduced Aβ load in the cortex and hippocampus

Aberrant APP processing leads to increased neurotoxic Aβ peptide deposition, with Aβ42 being the most toxic isoform. When we analyzed the levels of Aβ-42 in the different groups of mice, we found that TS +/+/+ mice presented enhanced levels of this peptide in the cortex (**figure 4A**) and hippocampus (**figure 4B**) but not in the cerebellum (**figure 4C**). Reducing the expression of Dyrk1A in TS animals reduced Aβ42 load in the cortex (ANOVA 'karyotype': $F_{(1,21)}$=17.73, p=0.001; 'Dyrk1A': $F_{(1,21)}$=2.15, p=0.16; ''karyotype' x 'Dyrk1A'': $F_{(1,21)}$=3.43, p=0.081**; figure 4A**).

In the hippocampus, although no significant differences were found between TS or CO mice carrying different number of copies of this gene ('karyotype': $F_{(1,21)}$=1.22, p=0.22; Dyrk1A': $F_{(1,21)}$=0.047, p=0.83), statistical analysis revealed that this was because reducing a copy of this gene in CO animals slightly increased the expression levels of Aβ-42 while it decreased them in TS animals (''karyotype' x 'Dyrk1A'': $F_{(1,21)}$=4.46, p=0.048; **figure 4B**).

This genetic manipulation did not modify of Aβ42 levels in the cerebellum of TS or CO animals ($F_{(1,21)}$=0.68, p=0.42; 'Dyrk1A': $F_{(1,21)}$=1.32, p=0.72; ''karyotype' x 'Dyrk1A'': $F_{(1,21)}$=0.74, p=0.40; **figure 4C**).

ACCEPTED MANUSCRIPT

Normalizing the *Dyrk1A* copy number reduced the levels of total tau found in the cortex, hippocampus and cerebellum of trisomic mice

Because abnormal tau accumulation and hyperphosphorylation are typical hallmarks implicated in the pathogenesis of AD, we first evaluated the effect of the *Dyrk1A* gene dose on the levels of this protein. Total tau expression (measured with the tau5 antibody) was increased in the cortex (ANOVA 'karyotype': $F_{(1,21)}$=34.54, p<0.001; **figure 5A**), hippocampus ($F_{(1,21)}$=23.18, p<0.001; **figure 5B**) and cerebellum ($F_{(1,21)}$=8.33, p=0.009; **figure 5C**) of TS +/+/+ mice. Reducing one functional copy of *Dyrk1A* reduced or normalized its levels of expression in the cortex ('Dyrk1A': $F_{(1,21)}$=2.06, p=0.16; ''karyotype' x 'Dyrk1A'': $F_{(1,21)}$=8.73, p=0.008) and cerebellum ('Dyrk1A': $F_{(1,21)}$=7.35, p=0.013; ''karyotype' x 'Dyrk1A'': $F_{(1,21)}$=8.95, p=0.007) of TS +/+/- mice and in the hippocampus of both TS +/+/- and CO +/- mice ($F_{(1,21)}$=33.07, p<0.001; ''karyotype' x 'Dyrk1A'': $F_{(1,21)}$=2.27, p=0.13).

Phosphorylated tau

Dyrk1A gene dosage and its protein expression levels have been previously linked to the hyperphosphorylation of tau. When we examined the phosphorylated state of tau, no differences were found in the amount of tau phosphorylation at the Ser202 residue in the cortex of the four groups of mice (ANOVA 'karyotype': $F_{(1,21)}$=2.80, p=0.11; 'Dyrk1A': $F_{(1,21)}$=0.00, p=0.96; ''karyotype' x 'Dyrk1A'': $F_{(1,21)}$=0.00, p=0.93; **figure 6A**) or at the Th212 residue ('karyotype': $F_{(1,21)}$=2.24, p=0.15; 'Dyrk1A': $F_{(1,21)}$=0.64, p=0.43; ''karyotype' x 'Dyrk1A'': $F_{(1,21)}$=0.58, p=0.45; **figure 7A**).

However, TS +/+/+ mice presented increased levels of phosphorylation of tau at Ser202 in the hippocampus and cerebellum, which were normalized after a reduction in the functional copy number of *Dyrk1A* (hippocampus: 'karyotype' $F_{(1,21)}$=7.09, p=0.016, 'Dyrk1A': $F_{(1,21)}$=14.85, p=0.001, ''karyotype' x 'Dyrk1A'': $F_{(1,21)}$=0.43, p=0.51, **figure 6B;** cerebellum**:** 'karyotype': $F_{(1,21)}$=0.55, p=0.46, 'Dyrk1A': $F_{(1,21)}$=70.23, p<0.001, ''karyotype' x 'Dyrk1A'', $F_{(1,21)}$=18.12, p<0.001**; figure 6C**).

In the case of the phosphorylation of tau at Thr212, TS +/+/+ mice did not differ from CO +/+ mice in the expression levels of this residue in the hippocampus or cerebellum, but a significant reduction in the expression levels of phosphorylation at the Thr212 residue was found in these structures (hippocampus: 'karyotype': $F_{(1,21)}$=3.99, p=0.063, 'Dyrk1A': $F_{(1,21)}$=35.04, p<0.001, ''karyotype' x 'Dyrk1A'': $F_{(1,21)}$=1.80, p=0.19; **figure 7B**; cerebellum: 'karyotype': $F_{(1,21)}$=0.16, p=0.68, 'Dyrk1A': $F_{(1,21)}$=2.10, p=0.16, ''karyotype' x 'Dyrk1A'': $F_{(1,21)}$=5.38, p=0.033, **figure 7C**) of TS +/+/- mice.

ACCEPTED MANUSCRIPT

Discussion

In the present study, normalizing the *Dyrk1A* gene dosage in aged trisomic mice normalized the density of senescent cells in the cingulate cortex, hippocampus and septum, prevented cholinergic neuron degeneration, and reduced APP expression in the hippocampus, Aβ load in the cortex and hippocampus, phosphorylated tau at the Ser202 residue in the hippocampus and cerebellum and the levels of total tau in the cortex, hippocampus and cerebellum.

Dyr1kA and cellular senescence

Cell senescence is a process that is characterized by permanent arrest of cell proliferation and that contributes to the dysfunction of the aging brain (Vidal *et al*., 2012). The number of senescent cells in tissues substantially increases during normal aging and increases oxidative stress, Aβ deposition and tau phosphorylation (Rodriguez-Sureda *et al*., 2015; He *et al*., 2013; Zhou *et al*., 2015; Kaluski *et al*., 2017). Fibroblasts with trisomy 21 present signs of premature cell senescence secondary to increased oxidative damage (Rodríguez-Sureda *et al*., 2015). Consistent with these findings, we have recently demonstrated that the hippocampus of adult TS mice present greater amounts of oxidative damage and an increased density of cells with a senescent phenotype (Parisotto *et al*., 2016). In addition, in the present study, an increased density of senescent cells was not only observed in the hippocampus but also in the septum and cingulate cortex of TS +/+/+ mice, and reducing the number of functional copies of *Dyrk1A* completely rescued this phenotype in these three structures. The septo-hippocampal cholinergic system in learning and attention (Bartus, 2000; Baxter and Chiba, 1999) and this population of neurons undergoes atrophy and degeneration in both AD and aging DS individuals (Mufson *et al*., 2003; 2000; Risser *et al*., 1997; Casanova *et al*., 1985; Godridge *et al*., 1987). In addition, the cingulate cortex and hippocampus, also implicated in learning and AD-related cognitive loss, present the increased accumulation of Aβ oligomers during disease progression (Serrano-Pozo et al., 2011). The results of the present study support a role for *Dyrk1A* during aging in these cell populations, which might aggravate neurodegenerative processes in AD and DS. However, future studies should investigate the mechanism by which the overexpression of this gene enhances cell senescence.

Role of *Dyrk1A* in cholinergic degeneration, APP and Aβ

Similar to that is found in DS and AD individuals, in the TS mouse, the number of cholinergic neurons in the basal prosencephalon progressively degenerates starting at the age of 6 months (Granholm *et al*., 2000; Hunter *et al*., 2004), playing a role in the cognitive decline that appears in both conditions. Consistent with these results, the present study demonstrated a reduced density of ChAT (the enzyme responsible for the biosynthesis of acetylcholine)-positive cells in the septum of 13-14 but not of 5-6-month-old TS +/+/+ mice. This neurodegeneration has been related to defects in retrograde transport of the neurotrophic growth factor (NGF) rather than the death of these neurons (Delcroix *et al*., 2004). Increased App expression disrupts NGF transport and causes cholinergic neuron degeneration (Salehi *et al*., 2006). In fact, Ts1Cje mice, which have a triplicated Mmu16 region without *App* triplication, do not show cholinergic system alterations (Chen *et al*., 2009), while *in vitro* studies in embryos from other models, carrying an extra copy of this gene, such as the Ts16 mouse (Fiedler *et al*., 1994; Opazo *et al*., 2006), present cholinergic deficits. Although the TS mouse carries an extra copy of the *App* gene, these mice do not develop amyloid plaques but display increased expression of full-length APP mRNA and APP protein in the cortex and hippocampus (Corrales *et al*., 2013; Seo and Isacson, 2005). Consistent with the evidence of the effect of APP on the cholinergic system degeneration, in the present study, we have found increased App protein levels in the cortex, hippocampus and cerebellum of TS +/+/+ mice.

ACCEPTED MANUSCRIPT

The cholinergic neurodegeneration found in DS and AD has been proposed to be induced by the formation of amyloid plaques and neurofibrillary tangles. Aβ deposition is an early event in AD that precedes neuronal degeneration and cognitive decline by several years or even decades (Cenini *et al*., 2012; Leverenz *et al*., 1998). A pathologic APP-dependent process for Aβ deposition occurs in the AD and DS brain. Overexpression of APP has been associated with an increase in Aβ42 levels in the brains of foetuses with DS (Teller *et al.*, 1996). Binding of aggregated Aβ to APP is likely to promote increased metabolic processing of APP through the amyloidogenic pathway, further contributing to Aβ deposition, neuritic degeneration, and synapse loss in AD (Bignante, 2013) and DS.

The hippocampal and cortical levels of Aβ42 have been demonstrated to be increased in TS mice at 4 months of age (Netzer *et al*., 2010) and this enhancement becomes more pronounced in later life stages (Corrales *et al*., 2013; Hunter *et al*., 2003), which may contribute to neuronal degeneration and cognitive alterations in TS mice. Additional evidence for the role of Aβ in cognitive degeneration originates from the demonstration that chronic treatment with Aβ-lowering drugs restores cognitive abilities in TS mice (Netzer *et al*., 2010). Natural and transgenic models of AD also display increases in APP and Aβ expression and support the hypothesis of the role of the amyloid cascade in AD pathogenesis. In addition, in normal rodents, some aspects of AD can be mimicked by intracerebral or intracerebroventricular infusion of Aβ peptides in the brain (Lawlor and Young, 2010), including AD-like behavioral alterations. In the present study, TS +/+/+ mice also displayed enhanced Aβ-42 levels in the cortex and hippocampus. However, the Aβ1-42 assessment was performed in guanidine hydrochloride extractions, where both soluble and insoluble Aβ1-42 species are present. Although TS mice express murine Aβ1-42 and do not form aggregates, a recent study has demonstrated increased expression of some low molecular weight oligomeric species in these animals (Sansevero et al., 2016), which are likely to play an important role in AD pathology in the absence of plaque pathology. Because soluble Aβ oligomers are key molecules involved in AD neuropathologyy (Ferreira et al., 2015), a detailed characterization of Aβ species should be performed by analyzing Aβ oligomers in different brain fractions (i.e. normal saline, SDS and guanidine hydrochloride).

We report here that normalizing the gene dosage of the *Dyrk1A* gene completely rescued ChAT levels in the aged TS +/+/- mice. Consistent with these results, Hijazi *et al*. (2013) demonstrated that downregulation of Dyrk1A by siRNA in cell lines derived from the cortex of Ts16 (Ctb) mice rescued ChAT expression to levels similar to those of normal cells.

Interestingly, the present study showed that reducing a functional copy of the *Dyrk1A* gene both in TS +/+/- and CO +/- mice also reduced APP protein levels in the cortex, hippocampus and cerebellum of these mice and Aβ42 levels in the cortex and hippocampus of TS +/+/- mice.

However, the reason for this positive effect in APP but not in Aβ-42 expression in CO+/- mice, as well as the lack of differences in cerebellar Aβ-42 levels between the four groups of mice in spite of changes in APP levels, remains unclear. The metabolism, processing or regulation of APP in the different brain structures might be different, but this and other mechanisms need to be further investigated.

Together, these studies propose *Dyrk1A* as a target gene involved in the normal function of the cholinergic system, possibly due to its effects on App expression and phosphorylation and on the formation of Aβ oligomers.

Implication of *Dyrk1A* in tau expression

ACCEPTED MANUSCRIPT

Increased tau levels in the brain have been reported to be neurotoxic and to promote neurodegeneration (Jin *et al*., 2011) because this protein is crucial in the promotion and stabilization of microtubule assembly. Abnormal tau expression and hyperphosphorylation are common features in AD and DS (Khatoon *et al*., 1994; Oyama *et al*., 1994), causing abnormalities in the cytoskeleton. In addition, increases in tau expression have been reported in other mouse models of AD and aging (Manich *et al*., 2011; Doehner *et al*., 2010; Madhusudan *et al*., 2009).

Classic intracellular NFTs are not present in the aging TS brain; however, extracellular tau deposits in aged TS mouse brains are higher (Rachubinski *et al*. 2012; Kern *et al*., 2011; Qian *et al*. 2013). In agreement with these results, in the present study, a significant elevation of total tau levels in the cortex, hippocampus and cerebellum of TS +/+/+ were found. However, alterations in the solubility of tau and phosphorylated tau are also crucial in the development of AD pathology in animal models that display increased expression of these proteins in the absence of neurofibrillary tangles. Therefore, future studies should assess, in TS mice, tau and phosphorylated tau levels in different brain fractions.

There is strong evidence that implicates the *DYRK1A*/*Dyrk1A* gene in the elevated tau expression found in DS and in the TS mouse. Wegiel *et al*. (2008) demonstrated a several-fold increase in the number of DYRK1A-positive NFTs in the brains of people with DS/AD than in the brains of people with only sporadic AD. In addition, a gene dosage-proportional increase in the level of DYRK1A in DS in the cytoplasm and the cell nucleus as well as enhanced cytoplasmic and nuclear immunoreactivity of DYRK1A were found (Wegiel *et al*., 2011).

Tau has also been demonstrated to be elevated in HEK-293 cells in which different isoforms of tau and Dyrk1A were co-expressed (Qian *et al*., 2013). These authors demonstrated that Dyrk1A enhanced tau expression in a dose-dependent manner and suggested that Dyrk1A enhances tau expression by stabilizing its mRNA.

Accordingly, in this study the *Dyrk1A* gene dosage also contributed to tau protein expression in a dose-dependent manner in TS mice; trisomic animals with three functional copies of this gene had higher levels of total tau than those with two copies of Dyrk1A.

Implication of *Dyrk1A* in tau hyperphosphorylation

Aberrant hyperphosphorylation of tau impairs its ability to bind microtubules (Billingsley and Kincaid, 1997), thus resulting in their disassembly (Alonso *et al*., 1996; 1994), tau self-assembly and formation of tau aggregates (Alonso *et al*., 2001).

The DYRK1A kinase has been involved in tau hyperphosphorylation and neurofibrillary degeneration. In fact, high levels of DYRK1A have been found in the cerebral cortex of patients with AD and DS (Ferrer *et al*., 2005). Moreover, aberrant phosphorylation of tau has also been reported in TS and Ts1Cje mice (Liu *et al*., 2008; Shukkur *et al*., 2006) and in CTb cells derived from the cerebral cortex of Ts16 animals (Cárdenas *et al*., 2012).

Hyperphosphorylation of tau at least 12 residues has been shown to be higher in AD brains (Yu *et al*. 2009). Among these residues two of them, Thr212 and Ser202, have received special attention.

DYRK1A phosphorylates tau at the Thr212 residue *in vitro* (Liu *et al*., 2008; Woods *et al*., 2001), in the brains of transgenic mice that overexpress the human DYRK1A protein (TgDYRK1A mice) (Ryoo *et al*., 2007) and in the brains of patients with AD (Morishima-Kawashima *et al*., 1995). DYRK1A also phosphorylates Ser202 (Ryoo *et al*., 2007), and the levels of phosphorylated tau at

ACCEPTED MANUSCRIPT

Ser202 are enhanced in the hippocampus and frontal cortex when DYRK1A levels are high. An increase in tau phosphorylated at Thr212 has also been observed in the hippocampus of old Tc1 mice compared with aged-matched control mice and young Tc1 mice (Sheppard *et al*., 2012). However, these authors did not find an increase in phosphorylation of tau at Ser202/Thr205 in the hippocampus of aged Tc1 mice.

In the present study, the levels of phosphorylation of tau at Ser202 were enhanced in the hippocampus and cerebellum of TS +/+/+ mice but not in the cortex. In addition, no significant elevations were found in the levels of phosphorylation of tau at Thr212 displayed by trisomic mice in any of the three structures.

Other studies have also failed to find increased tau phosphorylation at Thr212 in *Dyrk1A* cDNA-containing transgenic mice (Ferrer *et al*., 2005). The discrepancy between the data obtained in the present study or the study performed in TgDyrk1A cDNA mice (Ferrer *et al*., 2005) and the ones performed in the Tc1 (Sheppard *et al*., 2012) and the TgDYRK1A mice (Ryoo *et al*., 2007) may be due to the characteristics of the different models. While TS mice have triplicates of numerous mouse orthologous genes besides *Dyrk1A*, the Tc1 mouse carries a triplication of a larger number of human Hsa21 genes including *DYRK1A* but not *APP*. Thus, factors other than DYRK1A may contribute to the phosphorylation of tau at these sites, and may be differentially regulated in the two models. On the other hand, the differences found between the studies performed in Tg animals only overexpressing *Dyrk1A*/*DYRK1A* might be due to differences in the promoters used for the production of the transgenic mice; while one of them used the sheep metallothionein promoter that drives mouse Dyrk1A expression in cDNA transgenic mice (Altafaj *et al*., 2001), the other used the endogenous human promoter to drive expression of the human DYRK1A gene in TgDYRK1A mice (Ahn *et al*., 2006).

Thus, increased Dyrk1A activity by either overexpression or overactivation probably promotes neurofibrillary degeneration through hyperphosphorylation and/or elevated tau levels.

Interplay between *Dyrk1A*, Aβ and tau

Tau pathology in AD has been suggested to occur downstream of Aβ pathology, but the neurodegeneration initiated by Aβ is modulated by tau. An association between Aβ and hyperphosphorylated tau has been shown (Ribe *et al*., 2005; Oddo *et al*., 2003). Soluble Aβ can induce inactivation of phosphatases (Vogelsberg-Ragaglia *et al*., 2001) and activation of tau kinases (Hoshi *et al*., 2003; Otth *et al*., 2002), and promoting tau phosphorylation (Hoshi *et al*., 2003; Otth *et al*., 2002; Zheng *et al*., 2002) and the direct interaction between tau and Aβ induces tau aggregation and hyperphosphorylation (Rank *et al*., 2002). In addition, tau seems to be required for the neurotoxic effects of Aβ oligomers (Shipton *et al*., 2011). Knocking down endogenous tau prevents, whereas overexpression of human tau accelerates, the neuritic changes induced by Aβ oligomers (Jin *et al*., 2011). Tau knockout in transgenic mice has been reported to eliminate Aβ-induced neurotoxicity and behavioral deficits in animals (Ittner *et al*., 2010; Roberson *et al*., 2007).

As previously mentioned, *DYRK1A* plays an important role in tau overexpression and hyperphosphorylation and Aβ pathology in DS. DYRK1A mRNA and Aβ levels in the hippocampus are higher in patients with AD, transgenic mice and neuroblastoma cells (Kimura *et al*., 2007). In addition, Aβ induces an increase in the DYRK1A transcript, which leads to tau phosphorylation and overexpression of tau (Kimura *et al*., 2007). Thus, the upregulation of DYRK1A transcription resulting from Aβ overload further leads to tau phosphorylation, suggesting that DYRK1A could be a key molecule bridging β-amyloid production and tau phosphorylation in AD.

ACCEPTED MANUSCRIPT

A possible mechanism that has been proposed to account for the interplay between DYRK1A and APP is a positive feedback loop (see Cardenas *et al*., 2012) in which DYRK1A phosphorylates APP at Thr668 (Ryoo *et al*., 2008) favoring the amyloidogenic cleavage of APP (Judge *et al*., 2011; Lee *et al*., 2003), and Aβ42 induces an upregulation of DYRK1A (Kimura *et al*., 2007). The cooperative effects of these genes could affect tau expression and phosphorylation and result in abnormal expression and hyperphosphorylation, favouring tau aggregation and the destabilization of microtubules.

However, several studies in transgenic mice in which only the *Dyrk1A* gene is overexpressed or in trisomic mice that do not carry an extra functional copy of APP show tau pathology (Sheppard *et al*. 2012; Kimura *et al*., 2007). Thus, the enhanced phosphorylation observed in these models occurs independently of an extra copy of this gene, indicating that the activity of DYRK1A and other kinases may not need to interact with APP or Aβ to induce this hyperphosphorylation. In agreement with this hypothesis, Janel *et al*. (2004) described that AD patients exhibit a positive correlation between plasma DYRK1A levels and cerebrospinal fluid tau and phosphorylated tau proteins, but no correlation with Aβ42 levels.

Thus, although APP does not seem to be necessary for the appearance of some AD phenotypes, in its presence, the magnitude of neurodegeneration might be accelerated or aggravated. We propose here that the most likely mechanism for the different AD phenotypes found in TS mice is mediated by overexpression of *Dyrk1A*. Because Dyrk1A phosphorylates APP, and causes an increase in the amount of Aβ42, the increased level of Dyrk1A in TS brains might be responsible for the increased levels of total and hyperphosphorylated tau and of the elevated amounts of Aβ. These two mechanisms might interact to induce cellular senescence and cholinergic neurodegeneration, which is prevented after normalization of *Dyrk1A* gene dosage.

Conclusions

In conclusion, normalizing the gene dosage of *Dyrk1A* in the TS mouse rescued the density of senescent cells in the cingulate cortex, hippocampus and septum, prevented cholinergic neuron degeneration, and reduced APP expression in the hippocampus, Aβ load in the cortex and hippocampus, the expression of phosphorylated tau at the Ser202 residue in the hippocampus and cerebellum, and the levels of total tau in the cortex, hippocampus and cerebellum. Thus, the present study provides further support for the role of the *Dyrk1A* gene in several AD-like phenotypes found in TS mice and proposes that this gene could be a therapeutic target to treat AD in DS.

In this regard, several new molecules that inhibit DYRK1A activity have been proven to reduce some AD phenotypes such as tau expression or phosphorylation, APP levels or Aβ load (Kim *et al*., 2016; Abbassy *et al*., 2015; Contadeur *et al*., 2015). Future studies should test the efficacy of the only DYRK1A inhibitor that has been so far tested in humans, epigallocatechin-gallate (EGCG) (De la Torre *et al*., 2014; 2016) to prevent different AD-associated alterations.

ACCEPTED MANUSCRIPT

CAPTIONS

Figure 1. Representative images of β-galactosidase-positive cells in the hippocampus (A), medial septum (F) and cingulated cortex (I) of TS and CO mice with increased, normal or reduced copy number of the *Dyrk1A* gene. Means ± S.E.M. of the density of cells with a senescent phenotype in the GL (B), SGZ (D), medial septum (G) and cingulate cortex (J) and the total number of cells in the GC (C), SGZ (E), septum (H) and cingulate cortex (K) of the four groups of mice. *: p<0.05; **: p<0.01 TS +/+/+ vs. CO +/+; #: p<0.05, ##: p<0.01, ###: p<0.001 TS +/+/+ vs. TS +/+/- or CO +/+ vs. CO +/-. Bonferroni tests after significant ANOVAs.

Figure 2. Representative images of ChAT immunostaining in the medial septum of mice of 5-6 (A) and 13-14 months of age (B). Means ± S.E.M. of the density of ChAT+ cells in middle-aged (C) and aged (D) and the total number of ChAT+ cells in middle-aged (E) and aged (F) TS and CO mice with normal or reduced *Dyrk1A* gene dosage. *: p<0.05, **: p<0.01 TS +/+/+ vs. CO +/+; #: p<0.05, ###: p<0.001 TS +/+/+ vs. TS +/+/-. Bonferroni tests after significant ANOVAs.

Figure 3. Western blot analysis of APP immunoreactivity levels in the cortex (A), hippocampus (B) and cerebellum (C) of TS and CO mice with different dosages of *Dyrk1A*. GAPDH was used as an internal loading control. Blots were digitized, and the integrated optical density was estimated by densitometry. APP immunoreactivity changes in TS +/+/+, TS +/+/- and CO+/- animals were expressed relative to the values of CO +/+ mice (defined as 100% value). At least three independent gels were run for each sample. ***: p<0.001 TS +/+/+ vs. CO +/+. #: p<0.05; ##: p<0.01; ###: p<0.001 TS +/+/+ vs. TS +/+/- vs. TS +/+/- or CO +/+ vs. CO +/-. Bonferroni tests after significant ANOVAs.

Figure 4. Aβ42 levels in the cortex (A), hippocampus (B) and cerebellum (C) of TS +/+/+, TS +/+/-, CO +/+ and CO +/- mice. Data shown are the mean ± SEM (n=6 animals). * p<0.05; ** p<0.01 TS +/+/+ vs. CO +/+; #: p<0.05 TS +/+/+ vs. TS +/+/-. Bonferroni test after significant ANOVAs.

Figure 5. Representative images and western blot analysis of total tau (measured with the tau5 antibody) immunoreactivity levels in the cortex (A), hippocampus (B) and cerebellum (C) of TS and CO mice with different dosages of *Dyrk1A*. GAPDH was used as an internal loading control. Tau immunoreactivity changes in TS +/+/+, TS +/+/- and CO+/- animals were expressed relative to the values of CO +/+ mice (defined as 100% value). * p<0.05; ** p<0.01, ***: p<0.001 TS +/+/+ vs. CO +/+; #: p<0.05; ##: p<0.01; ###: p<0.001 TS +/+/+ vs. TS +/+/- or CO +/+ vs. CO +/-. Bonferroni test after significant ANOVAs.

Figure 6. Representative images and western blot analysis of pSer202 immunoreactivity levels in the cortex (A), hippocampus (B) and cerebellum (C) of TS and CO mice with different dosages of *Dyrk1A*. GAPDH was used as an internal loading control. Blots were digitized, and the integrated optical density was estimated by densitometry. Tau-pSer202 immunoreactivity changes in TS +/+/+, TS +/+/- and CO+/- animals were expressed relative to the values of CO +/+ mice (defined as 100% value). * p<0.05; ** p<0.01 TS vs. CO; #: p<0.05; ##: p<0.01 TS +/+/+ vs. TS +/+/- or CO +/+ vs. CO +/-. Bonferroni test after significant ANOVAs.

Figure 7. Representative images and western blot analysis of tau pThr212 immunoreactivity levels in the cortex (A), hippocampus (B) and cerebellum (C) of TS and CO mice with different dosages of *Dyrk1A*. GAPDH was used as an internal loading control. Blots were digitized, and the integrated optical density was estimated by densitometry. Tau-pThr212 immunoreactivity changes in TS

ACCEPTED MANUSCRIPT

+/+/+, TS +/+/- and CO+/- animals were expressed relative to the values of CO +/+ mice (defined as 100% value. #: p<0.05; ##: p<0.01 TS +/+/+ vs. TS +/+/- or CO +/+ vs. CO +/-. Bonferroni test after significant ANOVAs.

ACCEPTED MANUSCRIPT

ACCEPTED MANUSCRIPT

References

Abbassi R, Johns TG, Kassiou M, Munoz L. DYRK1A in neurodegeneration and cancer: molecular basis and clinical implications. Pharmacology and therapeutics. 2015; 151:87-98.

Ahn KJ, Jeong HK, Choi HS, Ryoo S-R, Kim YJ, Goo JS, Choi S-Y, Han J-S, Ha I, Song W-J. DYRK1A BAC transgenic mice show altered synaptic plasticity with learning and memory defects. Neurobiol Dis. 2006; 22: 463-472.

Alonso A, Zaidi T, Novak M, *et al*. Hyperphosphorylation induces self-assembly of tau into tangles of paired helical filaments/straight filaments. Proc Natl Acad Sci USA 2001; 98:6923-6928.

Alonso AC, Grundke-Iqbal I, Iqbal K. Alzheimer's disease hyperphosphorylated tau sequesters normal tau into tangles of filaments and disassembles microtubules. Nat Med 1996; 2:783-787.

Alonso AC, Zaidi T, Grundke-Iqbal I, *et al*. Role of abnormally phosphorylated tau in the breakdown of microtubules in Alzheimer disease. Proc Natl Acad Sci USA 1994; 91:5562-5566.

Altafaj X, Dierssen M, Baamonde C, Martí E, Visa J, Guimerá J, Oset M, Gonzalez JR, Flórez J, Fillat C, Estivill X. Neurodevelopmental delay, motor abnormalities and cognitive deficits in transgenic mice overexpressing Dyrk1A (minibrain), a murine model of Down's syndrome. Hum Mol Genet. 2001; 10: 1915-1923.

Bartesaghi R, Guidi S, Ciani E. Is it possible to improve neurodevelopmental abnormalities in Down syndrome? Rev Neurosci. 2011; 22: 419-455.

Bartus RT. On neurodegenerative diseases, models, and treatment strategies: lessons learned and lessons forgotten a generation following the cholinergic hypothesis: Exp Neurol. 2000; 163:495-529.

Baxter MG, Chiba AA. Cognitive functions of the basal forebrain: Curr Opin Neurobiol. 1999; 9: 178-183.

Becker W, Sippl W. Activation, regulation, and inhibition of DYRK1A. FEBS J. 2011; 278: 246-256.

Bignante EA, Heredia F, Morfini G, Lorenzo A. Amyloid β precursor protein as a molecular target for amyloid β-induced neuronal degeneration in Alzheimer's disease. Elsevier Neurobiol Aging. 2013; 34:2525–2537.

Billingsley ML, Kincaid RL. Regulated phosphorylation and dephosphorylation of tau protein: effects on microtubule interaction, intracellular trafficking and neurodegeneration. Biochem J 1997; 323: 577e591.

Bowes C, Li T, Frankel WN, Danciger M, Coffin JM, Applebury ML, Farber DB. Localization of a retroviral element within the rd gene coding for the beta subunit of cGMP phosphodiesterase. Proc Natl Acad Sci USA. 1993; 90: 2955-2959.

Cárdenas AM, Ardiles AO, Barraza N, Baéz-Matus X, Caviedes P. Role of tau protein in neuronal damage in Alzheimer's Disease and Down syndrome. Archives of Medical Research. 2012; 43: 645-654.

ACCEPTED MANUSCRIPT

Casanova MF, Walker LC, Whitehouse PJ, Price DL. Abnormalities of the nucleus basalis in Down's syndrome. Ann Neurol 1985; 18:310–313.

Cenini G, Dowling AL, Beckett TL, Barone E, Mancuso C, Murphy MP, *et al*. Association between frontal cortex oxidative damage and beta-amyloid as a function of age in Down syndrome. Biochim Biophys Acta. 2012; 1822:130-138.

Chen Y, Dyakin VV, *et al*. In vivo MRI identifies cholinergic circuitry deficits in a Down syndrome model. Neurobiol. Aging. 2009; 30:1453–1465.

Contadeur S, Benyamine H, Delalonde L, de Oliveira C, Leblond B, Foucourt A, Besson T, Casagrande AS, TAverne T, Girard A, Pando P, Désiré L. A novel DYRK1A inhibitor for the treatment of Alzheimer's disease: effect on tau and amyloid pathologies in vitro. Journal of Neurochemistry. 2015; 133:440-451.

Corrales A, Vidal R, García S, Vidal V, Martínez P, García E, *et al*. Chronic melatonin treatment rescues electrophysiological and neuromorphological deficits in a mouse model of Down syndrome. J Pineal Res. 2014; 56:51-61.

Corrales A, Martínez P, García S, Vidal V, García E, Flórez J, *et al*. Long-term oral administration of melatonin improves spatial learning and memory and protects against cholinergic degeneration in middle-aged Ts65Dn mice, a model of Down syndrome. J Pineal Res. 2013; 54: 346-58.

De la Torre R, de Sola S, Hernandez G, Farré M, Pujol J, Rodriguez J, Espadaler JM, Langohr K, Cuenca-Royo A, Principe A, Xicota L, Janel N, Catuara-Solarz S, Sanchez-Benavides G, Bléhaut H, Dueñas-Espín I, Del Hoyo L, Benejam B, Blanco-Hinojo L, Videla S, Fitó M, Delabar JM, Dierssen M; TESDAD study group.Safety and efficacy of cognitive training plus epigallocatechin-3-gallate in young adults with Down's syndrome (TESDAD): a double-blind, randomised, placebo-controlled, phase 2 trial. Lancet Neurol. 2016; 15:801-810.

De la Torre R, De Sola S, Pons M, Duchon A, de Lagran MM, Farré M, Fitó M, Benejam B, Langohr K, Rodriguez J, Pujadas M, Bizot JC, Cuenca A, Janel N, Catuara S, Covas MI, Blehaut H, Herault Y, Delabar JM, Dierssen M. Epigallocatechin-3-gallate, a DYRK1A inhibitor, rescues cognitive deficits in Down syndrome mouse models and in humans. Mol Nutr Food Res. 2014; 58:278-288.

Delcroix JD, Valletta J, *et al*.Trafficking the NGF signal: implications for normal and degenerating neurons. Prog. Brain Res. 2004; 146: 3–23.

Doehner J, Madhusudan A, Konietzko U, Fritschy J.-M, Knuesel I. Co-localization of reelin and proteolytic a beta pp fragments in hippocampal plaques in aged wild-type mice. J. Alzheimers Dis. 2010; 19:1339–1357.

Eikelenboom P, Veerhuis R, Scheper W, Rozemuller AJM, van Gool WA, Hoozemans JJM. The significance of neuroinflammation in understanding Alzheimer's disease. J Neural Transm. 2006; 113:1685–1695.

Ferrer I, Barrachina, M, *et al*. Constitutive Dyrk1A is abnormally expressed in Alzheimer disease, Down syndrome, Pick disease, and related transgenic models. Neurobiol Dis. 2005; 20:392–400.

ACCEPTED MANUSCRIPT

Ferreira ST, Lourenco MV, Oliveira MM, De Felice FG. Soluble amyloid-beta oligomers as synaptotoxins leading to cognitive impairment in Alzheimer's disease. Front. Cell. Neurosci. 2015; 9, 191.

Fiedler JL, Epstein CJ. Regional alteration of cholinergic function in central neurons of trisomy 16 mouse fetuses, an animal model of human trisomy 21 (Down syndrome). Brain Res. 1994; 658:27–32.

Fotaki V, Dierssen M, Alcántara S, Martínez S, Martí E, Casas C, Visa J, Soriano E, Estivill X, Arbonés ML. Dyrk1A haploinsufficiency affects viability and casues developmental delay and abnormal brain morphology in mice. Mol Cell Biol. 2002; 22: 6636-6647.

Franklin KBJ, Paxinos G. The mouse brain in stereotaxic coordinates. 1997. San Diego: Academic Press.

Godridge H, Reynolds GP, Czudek C, Calcutt NA, Benton M. Alzheimer-like neurotransmitter deficits in adult Down's syndrome brain tissue: J Neurol Neurosurg Psychiatry 1987; 50:775-778.

Granholm AC, Sanders LA, Crnic LS. Loss of cholinergic phenotype in basal forebrain coincides with cognitive decline in a mouse model of Down's syndrome. Exp Neurol. 2000; 161:647-63.

Guedj F, Lopes Pereira P, Najas S, Barallobre M-J, Chabert C, Souchet B, Sebrie C, Verney C, Herault Y, Arbonés M, Delabar JM. DYRK1A: A master regulatory protein controlling brain growth. Neurobiol Dis. 2012; 46: 190-203

Hardy JA, Higgins GA. Alzheimer's disease: the amyloid cascade hypothesis. Science. 1992; 256:184-185.

Hardy J. Has the amyloid cascade hypothesis for Alzheimer's disease been proved? Curr Alzheimer Res. 2006; 3:71-73.

Haydar TF, Reeves RH. Trisomy 21 and early brain development. Trends Neurosci. 2012; 35:81-91.

He N, Jin WL, Lok KH, *et al*. Amyloid-β(1-42) oligomer accelerates senescence in adult hippocampal neural stem/progenitor cells via formylpeptide receptor 2. Cell Death Dis. 2013; 4:e924.

Hijazi M, Fillat C, Medina JM, Velasco A. Overexpression of DYRK1A inhibits choline acetyltransferase induction by oleic acid in cellular models of Down syndrome. Exp Neurol. 2013; 239: 229-234.

Hoshi M, Sato M, Matsumoto S, *et al*. Spherical aggregates of betaamyloid (amylospheroid) show high neurotoxicity and activate tau protein kinase I/glycogen synthase kinase-3beta. Proc Natl Acad Sci USA. 2003; 100:6370-6375.

Hunter CL, Bachman D, Granholm AC. Minocycline prevents cholinergic loss in a mouse model of Down's syndrome. Ann Neurol. 2004; 56:675-88.

ACCEPTED MANUSCRIPT

Hunter CL, Isacson O, Nelson M, Bimonte-Nelson H, Seo H, Lin L, *et al*. Regional alterations in amyloid precursor protein and nerve growth factor across age in a mouse model of Down's syndrome. Neurosci Res. 2003; 45:437-445.

Ittner LM, Ke YD, Delerue F, Bi M, Gladbach A, van Eersel J, Wolfing H, Chieng BC, Christie MJ, Napier IA, Eckert A, Staufenbiel M, Hardeman E, Gotz J. Dendritic function of tau mediates amyloid-beta toxicity in Alzheimer's disease mouse models. Cell. 2010; 142:387-397.

Janel N, Sarazin M, Corlier F, Corne H, de Souza LC, Hamelin L, Aka A, Lagarde J, Blehaut H, Vindié V, Rain JC, Arbones ML, Dubois B, Potier MC, Bottlaender M, Delabar JM. Plasma DYRK1A as a novel risk factor for Alzheimer's disease. Transl Psychiatry. 2014; 4: e425.

Jin M, Shepardson N, Yang T, Chen G, Walsh D, Selkoe DJ. Soluble amyloid beta-protein dimers isolated from Alzheimer cortex directly induce Tau hyperphosphorylation and neuritic degeneration. Proc Natl Acad Sci U S A. 2011; 108: 5819-5824.

Judge M, Hornbeck L, Potter H, *et al*. Mitosis-specific phosphorylation of amyloid precursor protein at threonine 668 leads to its altered processing and association with centrosomes. Mol Neurodegener. 2011; 6:80.

Kaluski S, Portillo M, Bernard A, Stein D, Einav M, ZhongL, Ueberham U, Arendt T, Mostoslavsky R, Sahay A, Toiber D. Neuroprotective functions for the histone deacetylase SIRT6. Cell Reports. 2017; 18: 3052-3062.

Kern DS, Maclean KN, Jiang H, Synder EY, Sladek JR, Bjugstad KB. Neural stem cells reduce hippocampal tau and reelin accumulation in aged ts65dn Down syndrome mice. Cell Transplant. 2011; 20:371–379.

Khatoon S, Grundke-Iqbal I, Iqbal K (1994) Levels of normal and abnormally phosphorylated tau in different cellular and regional compartments of Alzheimer disease and control brains. FEBS Lett. 1994; 351: 80-84.

Kim H, Lee KS, Kim AK, Choi M, Choi K, Kang M, Chi SW, Lee MS, Lee JS, Lee SY, Song WJ, Yu K, Cho S. A chemical with proven clinical safety rescues Down-syndrome-related phenotypes in through DYRK1A inhibition. Disease models and mechanisms. 2016: 9: 839-848.

Kimura R, Kamino K, Yamamoto M, Nuripa A, Kida T, Kazui H, Hashimoto R, Tanaka T, Kudo T, Yamagata H, Tabara Y, Miki T, Akatsu H, Kosaka K, Funakoshi E, Nishitomi K, Sakaguchi G, Kato A, Hattori H, Uema T, Takeda M. The DYRK1A gene, encoded in chromosome 21 Down syndrome critical region, bridges between beta-amyloid production and tau phosphorylation in Alzheimer disease. Hum Mol Genet. 2007; 16:15-23.

Lawlor P, Young D. Ab infusion and related models of Alzheimer dementia. In: De Deyn P, Van Dam D, editors. Animal Models of Dementia. New York: Springer Science and Business Media; 2010. p. 347-370.

Lee MS, Kao SC, Lemere CA, Xia W, Tseng HC, Zhou Y, Neve R, Ahlijanian MK, Tsai LH. APP processing is regulated by cytoplasmic phosphorylation: J Cell Biol. 2003; 163:83-95.

ACCEPTED MANUSCRIPT

Leverenz JB, Raskind MA. Early amyloid deposition in the medial temporal lobe of young Down syndrome patients: a regional quantitative analysis. Exp Neurol. 1998; 150:296–304.

Liu F, Liang Z, Wegiel J, Hwang YW, Iqbal K, Grundke-Iqbal I, Ramakrishna N, Gong CX. Overexpression of Dyrk1A contributes to neurofibrillary degeneration in Down syndrome. FASEB J. 2008; 22: 3224-3233.

Liu DP, Schmidt C, Billings T, Davisson MT. A quantitative PCR genotyping assay for the Ts65Dn mouse model of Down syndrome. Biotechniques. 2003; 35: 1170-1174.

Lockrow J, Boger H, Bimonte-Nelson H, Granholm AC. Effects of long-term memantine on memory and neuropathology in Ts65Dn mice, a model for Down syndrome. Behav Brain Res. 2011; 221: 610-22.

Lockrow J, Prakasam A, Huang P, Bimonte-Nelson H, Sambamurti K, Granholm AC. Cholinergic degeneration and memory loss delayed by vitamin E in a Down syndrome mouse model. Exp Neurol. 2009; 216: 278-89.

Lott IT. Neurological phenotypes for Down syndrome across the life span. Prog Brain Res. 2012; 197:101-21.

Lott IT, Dierssen M. Cognitive deficits and associated neurological complications in individuals with Down's syndrome. Lancet Neurol. 2010; 9:623-33.

Ma QL, Yang F, Rosario ER, *et al*. Beta-amyloid oligomers induce phosphorylation of tau and inactivation of insulin receptor substrate via c-Jun N-terminal kinase signaling: suppression by omega-3 fatty acids and curcumin. J Neurosci 2009; 29:9078-9089.

Madhusudan A, Sidler C, Knuesel I. Accumulation of reelin-positive plaques is accompanied by a decline in basal forebrain projection neurons during normal aging. Eur. J. Neurosci. 2009; 30: 1064–1076.

Manich G, Mercader C, del Valle J, Duran-Vilaregut J, Camins A, Pallas M, Vilaplana J, Pelegri C. Characterization of amyloid-beta granules in the hippocampus of samp8 mice. J. Alzheimers Dis. 2011; 25:535–546.

Millan Sanchez M, Heyn SN, Das D, Moghadam S, Martin KJ, Salehi A. Neurobiological elements of cognitive dysfunction in down syndrome: exploring the role of APP. Biol Psychiatry. 2012; 71: 403-409.

Mufson EJ, Cochran E, Benzing W, Kordower JH. Galaninergic innervation of the cholinergic vertical limb of the diagonal band (Ch2) and bed nucleus of the stria terminalis in aging, Alzheimer's disease, and Down's syndrome. Dementia. 1993; 4: 237–250.

Mufson EJ, Ma SY, Cochran EJ, *et al*. Loss of nucleus basalis neurons containing trkA immunoreactivity in individuals with mild cognitive impairment and early Alzheimer's disease. J Comp Neurol 2000; 427: 9–30.

Murphy MP and LeVine, H. Alzheimer’s Disease and the β-Amyloid Peptide. J Alzheimers Dis 2010; 19(1): 311.

ACCEPTED MANUSCRIPT

Netzer WJ, Powell C, Nong Y, Blundell J, Wong L, Duff K, *et al*. Lowering beta-amyloid levels rescues learning and memory in a Down syndrome mouse model. PLoS One. 2010; 5: e10943.

Oddo S, Caccamo A, Kitazawa M, *et al*. Amyloid deposition precedes tangle formation in a triple transgenic model of Alzheimer's disease. Neurobiol Aging 2003; 24:1063e1070.

Opazo P, Saud K, *et al*. Knockdown of amyloid precursor protein normalizes cholinergic function in a cell line derived from the cerebral cortex of a trisomy 16 mouse: an animal model of Down syndrome. J Neurosci Res. 2006; 84: 1303–1310.

Otth C, Concha II, Arendt T, *et al*. AbetaPP induces cdk5-dependent tau hyperphosphorylation in transgenic mice Tg2576. J Alzheimers Dis. 2002; 4:417-430.

Oyama F, Cairns NJ, Shimada H, Oyama R, Titani K, Ihara Y. Down's syndrome: Up-regulation of beta-amyloid protein precursor and tau mRNAs and their defective coordination. J Neurochem. 1994; 62: 1062-1066.

Parisotto EB, Vidal V, García-Cerro S, Lantigua S, Wilhelm Filho D, Sanchez-Barceló EJ, Martínez-Cué C, Rueda N. Chronic melatonin administration reduced oxidative damage and cellular senescence in the hippocampus of a mouse model of Down syndrome. Neurochem Res. 2016; in press.

Park J, Chung KC. New Perspectives of Dyrk1A Role in Neurogenesis and Neuropathologic Features of Down Syndrome. Exp Neurobiol. 2013; 22: 244-248. Salehi A, Delcroix JD, *et al*. Increased App expression in a mouse model of Down's syndrome disrupts NGF transport and causes cholinergic neuron degeneration. Neuron. 2006;
51:29–42.

Paxinos G, Watson C. The rat brain in stereotaxic coordinates. 2007. Academic Press, NY. 6th Edition.

Qian W, Jin N, Shi J, Yin X, Jin X, Wang S, Cao M, Iqbal K, Gong CX, Liu F. Dual-specificity tyrosine phosphorylation-regulated kinase 1A (Dyrk1A) enhances tau expression: J Alzheimers Dis. 2013; 37: 529-538.

Rachubinski AL, Crowley SK, Sladek JR, Maclean KN, Bjugstad KB. Effects of neonatal neural progenitor cell implantation on adult neuroanatomy and cognition in the ts65dn model of Down syndrome. PLoS One. 2012; 7: e36082.

Rank KB, Pauley AM, Bhattacharya K, *et al*. Direct interaction of soluble human recombinant tau protein with Abeta 1-42 results in tau aggregation and hyperphosphorylation by tau protein kinase II. FEBS Lett. 2002; 514:263-268.

Ribe EM, Perez M, Puig B, *et al*. Accelerated amyloid deposition, neurofibrillary degeneration and neuronal loss in double mutant APP/tau transgenic mice. Neurobiol Dis 2005; 20:814e822.

Risser D, Lubec G, Cairns N, Herrera-Marschitz M. Excitatory amino acids and monoamines in parahippocampal gyrus and frontal cortical pole of adults with Down syndrome: Life Sci. 1997; 60: 1231-1237.

ACCEPTED MANUSCRIPT

Roberson ED, Scearce-Levie K, Palop JJ, Yan F, Cheng IH, Wu T, Gerstein H, Yu GQ, Mucke L. Reducing endogenous tau ameliorates amyloid beta-induced deficits in an Alzheimer's disease mouse model. Science. 2007; 316: 750-754.

Rodríguez-Sureda V, Vilches Á, Sánchez O, *et al*. Intracellular oxidant activity, antioxidant enzyme defense system, and cell senescence in fibroblasts with trisomy 21. Oxid Med Cell Longev 2015; 2015:509241.

Rueda N, Flórez J, Martínez-Cué C. Mouse models of Down syndrome as a tool to unravel the causes of mental disabilities. NeuralPlasticity. 2012: 584071.

Rueda N, Llorens-Martín M, Flórez J, Valdizán E, Banerjee P, Trejo JL, *et al*. Memantine normalizes several phenotypic features in the Ts65Dn mouse model of Down syndrome. J Alzheimers Dis. 2010; 21: 277-90.

Ryoo SR, Cho HJ, Lee HW, Jeong HK, Radnaabazar C, Kim YS, Kim MJ, Son MY, Seo H, Chung SH, Song WJ. Dual-specificity tyrosine(Y)-phosphorylation regulated kinase 1A-mediated phosphorylation of amyloid precursor protein: evidence for a functional link between Down syndrome and Alzheimer's disease: J Neurochem. 2008; 104: 1333-1344.

Ryoo SR, Jeong HK, Radnaabazar C, Yoo JJ, Cho HJ, Lee HW, Kim IS, Cheon YH, Ahn YS, Chung SH, Song WJ. DYRK1A-mediated hyperphosphorylation of Tau. A functional link between Down syndrome and Alzheimer disease: J Biol Chem. 2007; 282: 34850-34857.

Sabbagh MN, Fleisher A, Chen K, Rogers J, Berk C, Reiman E, *et al*. Positron emission tomography and neuropathologic estimates of fibrillar amyloid-β in a patient with Down syndrome and Alzheimer disease. Arch Neurol. 2011; 68:1461-6.

Sansevero G, Begenisic T, Mainardi M, Sale A. Experience-dependent reduction of soluble β-amyloid oligomers and rescue of cognitive abilities in middle-age Ts65Dn mice, a model of Down syndrome. Exp Neurol. 2016; 283: 49-56.

Seo H, Isacson O. Abnormal APP, cholinergic and cognitive function in Ts65Dn Down's model mice. Exp Neurol. 2005; 193:469-80.

Serrano-Pozo A, Frosch MP, Masliah E, Hyman BT. Neuropathological alterations in Alzheimer Disease. Cold Spring Harb Perspect Med. 2011; 1:a006189.

Sheppard O, Plattner F, Rubin A, Slender A, Linehan JM, Brandner S, Tybulewicz VL, Fisher EM, Wiseman FK. Altered regulation of tau phosphorylation in a mouse model of down syndrome aging: Neurobiol Aging. 2012; 33: 828:31-44.

Shin M, Besser LM, Kucik JE, Lu C, Siffel C, Correa A, *et al*. Prevalence of Down syndrome among children and adolescents in 10 regions of the United States. Pediatrics. 2009; 124:1565-71.

Shipton OA, Leitz JR, Dworzak J, *et al*. Tau protein is required for amyloid {beta}-induced impairment of hippocampal long-term potentiation. J Neurosci. 2011; 31:1688-1692.

ACCEPTED MANUSCRIPT

Shukkur EA, Shimohata A, Akagi T, Yu W, Yamaguchi M, Murayama M, Chui D, Takeuchi T, Amano K, Subramhanya KH, Hashikawa T, Sago H, Epstein CJ, Takashima A, Yamakawa K. Mitochondrial dysfunction and tau hyperphosphorylation in Ts1Cje, a mouse model for Down syndrome. Hum Mol Genet. 2006; 15:2752-62.

Sipos E, Kurunczi A, Kasza A, Horváth J, Felszeghy K, Laroche S, *et al*. Beta-amyloid pathology in the entorhinal cortex of rats induces memory deficits: implications for Alzheimer's disease. Neuroscience. 2007; 147:28-36.

Smith DJ, Stevens ME, Sudanagunta SP, Bronson RT, Makhinson M, Watabe AM, O'Dell TJ, Fung J, Weier HU, Cheng JF, Rubin EM. Functional screening of 2 Mb of human chromosome 21q22.2 in transgenic mice implicates minibrain in learning defects associated with Down syndrome. Nat Genet. 1997; 16: 28-36.

Sturgeon X, Gardiner KJ. Transcript catalogs of human chromosome 21 and orthologous chimpanzee and mouse regions. Mamm Genome. 2011; 22: 261-71.

Teipel SJ, Hampel H. Neuroanatomy of Down syndrome in vivo: a model of preclinical Alzheimer's disease. Behav Genet. 2006; 36: 405–15.

Tejedor FJ, Hämmerle B. MNB/DYRK1A as a multiple regulator of neuronal development. FEBS J. 2011; 278: 223-235.

Teller JK, Russo C, DeBusk LM, Angelini G, Zaccheo D, Dagna-Bricarelli F, Scartezzini P, Bertolini S, Mann DM, Tabaton M, Gambetti P. Presence of soluble amyloid beta-peptide precedes amyloid plaque formation in Down's syndrome. Nat Med. 1996; 2:93-5.

Trejo JL, Carro E, Torres-Aleman I. Circulating insulin-like growth factor I mediates exercise-induced increases in the number of new neurons in the adult hippocampus. J Neurosci. 2001; 21:1628-1634.

Vidal MA, Walker NJ, Napoli E, *et al*. Evaluation of senescence in mesenchymal stem cells isolated from equine bone marrow, adipose tissue, and umbilical cord tissue. Stem Cells Dev. 2012; 21: 273–283.

Vingtdeux V, Hamdane M, Gompel M, Begard S, Drobecq H, Ghestem A, Grosjean MV, Kostanjevecki V, Grognet P, Vanmechelen E, Buee L, Delacourte A, Sergeant N. Phosphorylation of amyloid precursor carboxy-terminal fragments enhances their processing by a gamma-secretase-dependent mechanism: Neurobiol Dis. 2005; 20:625-37.

Vogelsberg-Ragaglia V, Schuck T, Trojanowski JQ, *et al*. PP2A mRNA expression is quantitatively decreased in Alzheimer's disease hippocampus. Exp Neurol. 2001; 168:402e412.

Wegiel J, Gong CX, Hwang YW. The role of DYRK1A in neurodegenerative diseases: FEBS J. 2011; 278: 236-45.

Wegiel J, Dowjat K, Kaczmarski W, Kuchna I, Nowicki K, Frackowiak J, Mazur Colecka B, Wegiel J. The role of overexpressed DYRK1A protein in the early onset of neurofibrillary degeneration in Down syndrome. Acta Neuropathol. 2008; 116: 391-407.

ACCEPTED MANUSCRIPT

Wilcock DM, Griffin WS. Down's syndrome, neuroinflammation, and Alzheimer neuropathogenesis. J Neuroinflammation. 2013; 10:84.

Wilcock DM. Neuroinflammation in the aging down syndrome brain; Lessons from Alzheimer's disease. Curr Gerontol Geriatr Res. 2012; 1–10.

Woods YL, Cohen P, Becker W, Jakes R, Goedert M, Wang X, Proud CG. The kinase DYRK phosphorylates protein-synthesis initiation factor eIF2Bepsilon at Ser539 and the microtubule-associated protein tau at Thr212: potential role for DYRK as a glycogen synthase kinase 3-priming kinase: Biochem J. 2001; 355: 609-615.

Yu Y, Run X, Liang Z, Li Y, Liu F, Liu Y, Iqbal K, Grundke-Iqbal I, Gong CX. Developmental regulation of tau phosphorylation, tau kinases and tau phosphatases. J Neurochem. 2009; 108: 1480-1494.

Zheng WH, Bastianetto S, Mennicken F, *et al*. Amyloid beta peptide induces tau phosphorylation and loss of cholinergic neurons in rat primary septal cultures. Neuroscience. 2002; 115:201-211.

ACCEPTED MANUSCRIPT

ACCEPTED MANUSCRIPT

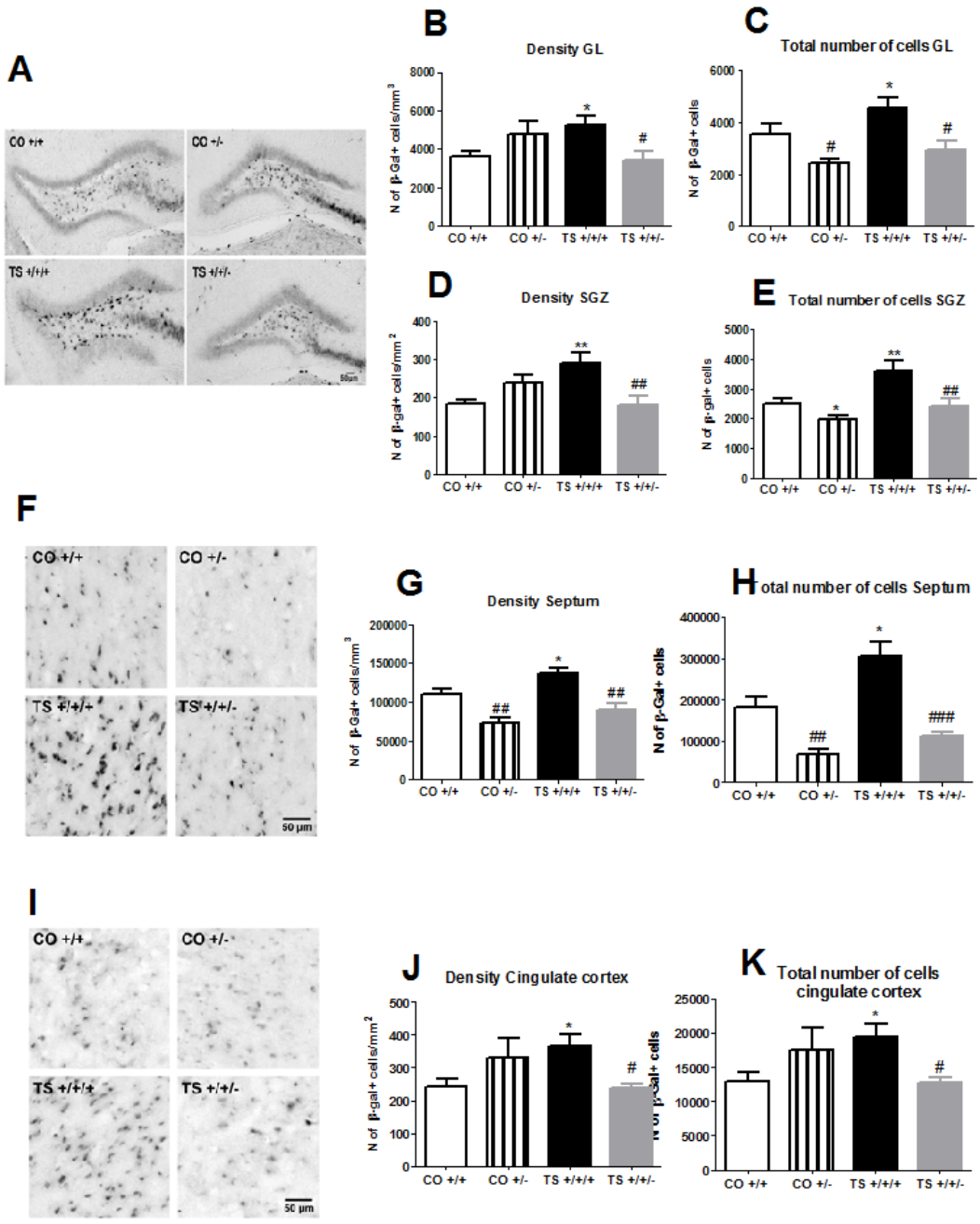

Fig. 1

ACCEPTED MANUSCRIPT

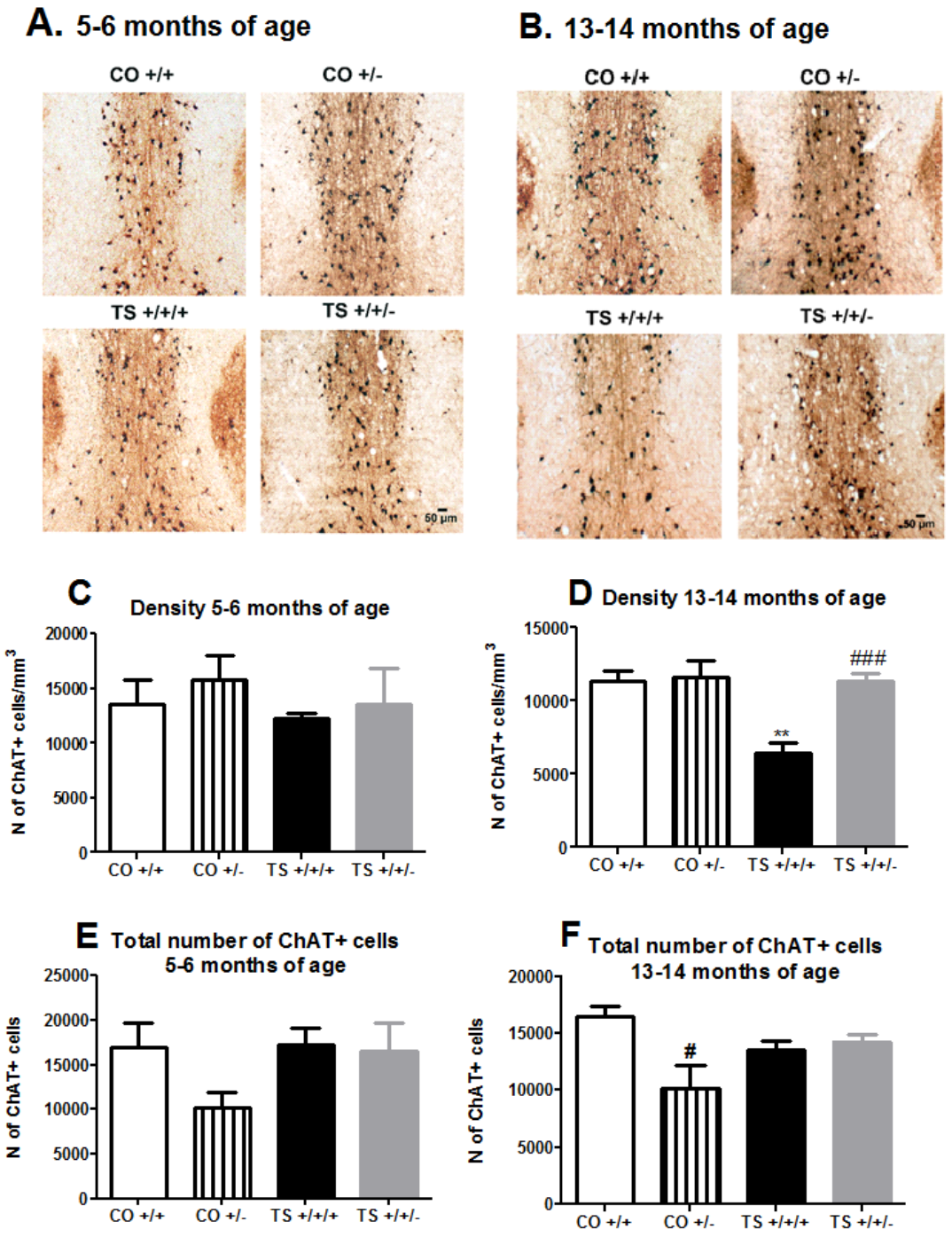

Fig. 2

ACCEPTED MANUSCRIPT

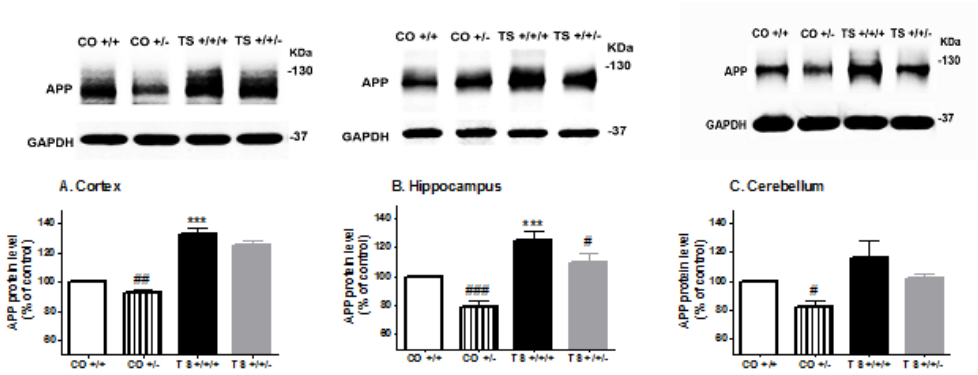

Fig. 3

ACCEPTED MANUSCRIPT

ACCEPTED MANUSCRIPT

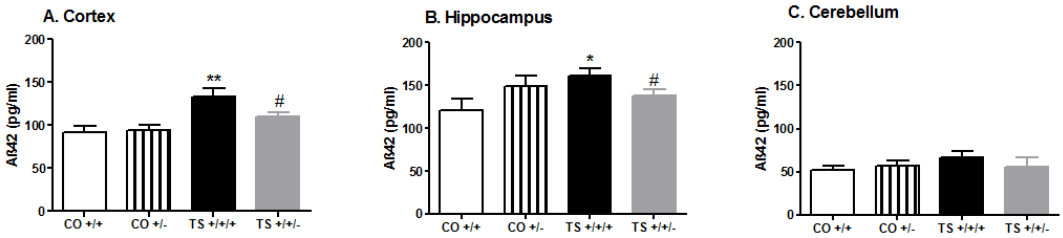

Fig. 4

ACCEPTED MANUSCRIPT

ACCEPTED MANUSCRIPT

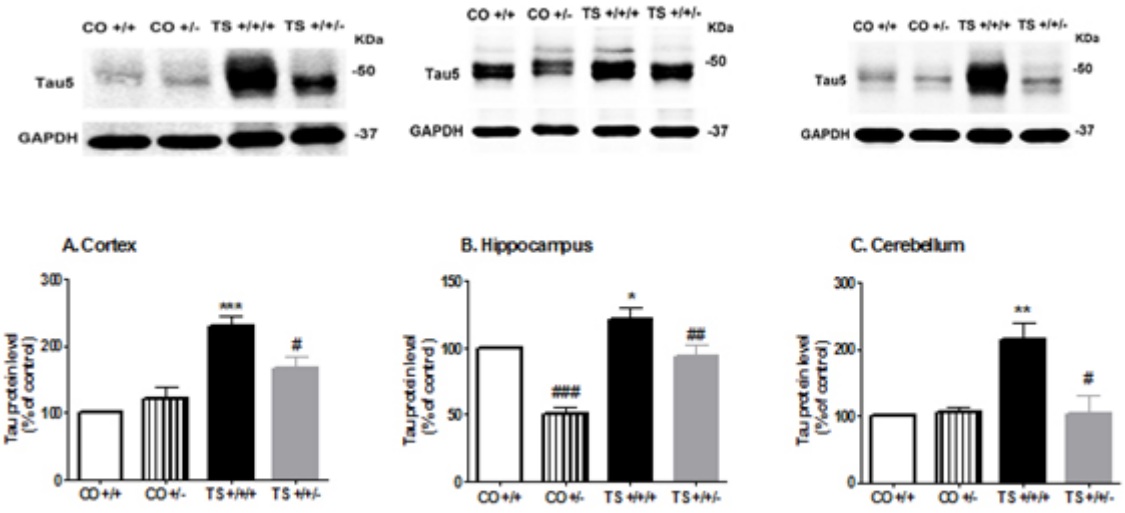

Fig. 5

ACCEPTED MANUSCRIPT

ACCEPTED MANUSCRIPT

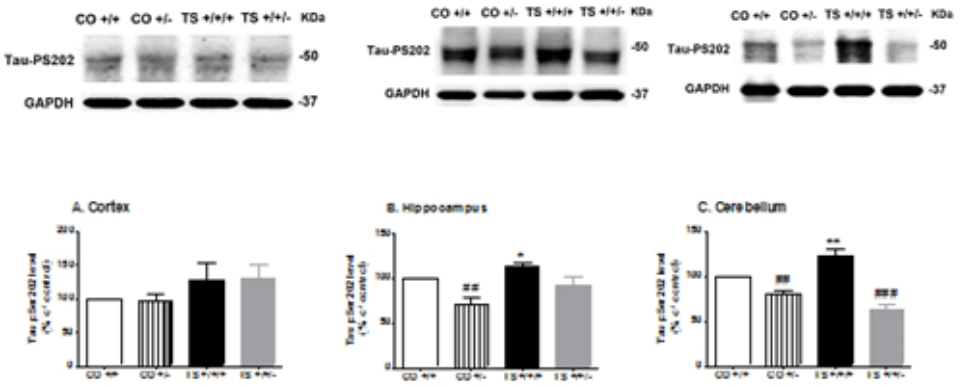

Fig. 6

ACCEPTED MANUSCRIPT

ACCEPTED MANUSCRIPT

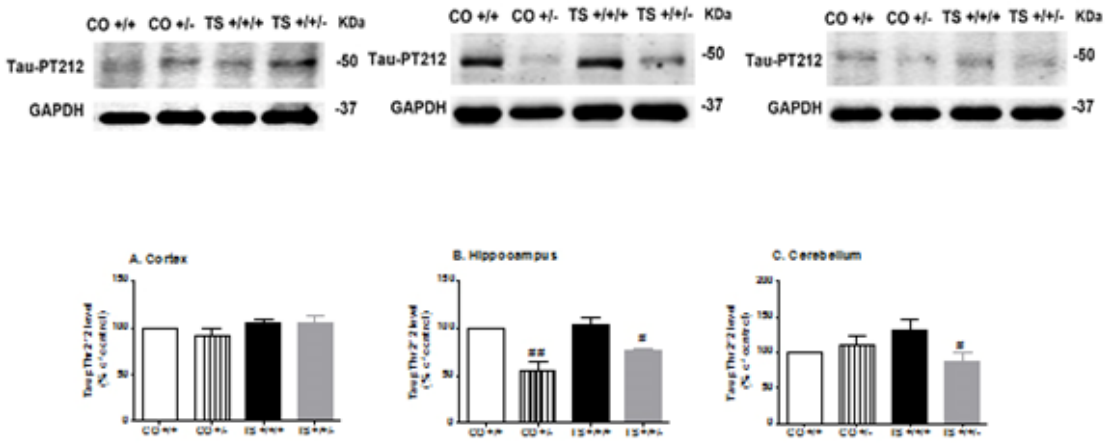

Fig. 7

ACCEPTED MANUSCRIPT